31st Annual International Conference of the IEEE EMBS
Minneapolis, Minnesota, USA, September 2-6, 2009

Imaging Mass Spectrometry Analysis for Follicular Lymphoma Grading

Siddharth S. Samsi, Ashok K. Krishnamurthy, M. Reid Groseclose, Richard M. Caprioli, Gerard Lozanski and Metin N. Gurcan, Senior Member IEEE

Abstract—**Follicular lymphoma (FL) is the second most common non-Hodgkins lymphoma in the United States. While the current diagnosis depends heavily on the review of H&E-stained tissues, additional sources of information such as IHC are occasionally needed. Matrix-assisted laser desorption/ionization mass spectrometry (MALDI-MS) can be used to generate protein profiles from localized tissue regions, thus making it possible to relate changes in tissue histology to the changes in the protein signature of the tissue. It may be possible to determine potential biomarkers that can indicate disease state and prognosis based on the protein profile. This research aims to combine two different but related types of data in order to develop a unique diagnosis methodology that can potentially improve the accuracy of diagnosis. Preliminary analysis has shown promising results for distinguishing intrafollicle regions from the mantle and follicle zones in normal tissue.**

I. Introduction

Follicular lymphoma (FL) is the second most common non-Hodgkin's lymphoma in the United States, accounting for 35% of all adult B cell lymphomas, and 70% of low grade lymphomas in U.S. clinical trials. Although reliable clinical risk stratification tools are available for FL, the optimal choice of treatment continues to depend heavily on morphology-based histological grading. In a system adopted by the World Health Organization (WHO), follicular lymphomas are stratified into three grades depending on the average count of centroblasts (noncleaved follicular center cells) in ten, randomly selected, standard high-power fields (HPF) [1]. Follicular lymphomas with low histological grades (I and II) are considered incurable with currently available therapies, however, high-grade follicular lymphomas (Grade III) may be cured with aggressive chemotherapy. Currently, the inter-reader agreement between pathologists in grading FL is extremely low: in a multi-site study, the agreement among experts for the various grades of follicular lymphoma varied between 61% and 73% [2]. These grade-related differences underscore the need for a precise and reproducible system for the histological grading of FL.

Computer aided diagnosis tools for grading of Follicular Lymphoma are being developed by our group [3]. In the approach in [4] Hematoxylin and Eosin (H&E) and immunohistochemical (IHC) stained tissue images are morphologically analyzed to develop statistical models for detecting follicles and centroblasts. Research described in [3] is based upon this work, and constructs models used to describe the tissue histology in order to classify histological grades of FL. This research has demonstrated the potential to reduce errors in the classification of FL.

While the current diagnosis heavily depends on the review of H&E-stained tissues, additional sources of information such as IHC stained images are frequently needed. In order to better quantify the information inherent in the tissue, we have used a relatively new technology called imaging mass spectrometry (IMS). IMS has emerged as a powerful tool for studying the spatial arrangement of proteins, peptides, lipids, and small molecules in tissues [5-6]. The multichannel detection capability of mass spectrometry (MS) enables the position sensitive analysis of hundreds of different molecules in a single experiment. This is achieved by acquiring mass spectra across a sample at precisely defined geometrical coordinates. Post acquisition processing of the data enables ion density maps (images) to be generated for any of the detected species where the relative intensity of the ions is displayed based on a color intensity scale [7].

IMS can provide localized protein profiles from a tissue, thus making it possible to relate changes in tissue histology to the changes in the protein signature of the sample. By comparing spectra from normal and diseased tissue, it is possible to determine potential biomarkers that can indicate the presence/absence of disease [8-9] and may also be used to determine disease progression and patient prognosis [10]. A histology guided approach using MALDI-MS profiling has also been used for proteomic analysis of specific tissues sites [11-13] and for classifying tissue samples into different cancer types.

In this paper we describe a unique methodology that can potentially improve the accuracy of FL diagnosis by using MS data to classify a tissue into disease relevant morphological sections.

S. Samsi is with the Ohio Supercomputer Center, USA (phone: 614-247-8174; fax: 614-292-7168; e-mail: samsi@osc.edu).

A.K. Krishnamurthy, is with the Ohio Supercomputer Center, USA (e-mail: ashok@osc.edu).

R.M. Caprioli is with the Vanderbilt University School of Medicine (e-mail: Richard.m.caprioi@vanderbilt.edu)

M.R. Groseclose is with the Vanderbilt University School of Medicine (e-mail: reid.groseclose@vanderbilt.edu)

G. Lozanski is with the Department of Pathology, The Ohio State University Medical Center (gerard.lozanski@osumc.edu)

M. N. Gurcan is with the Department of Biomedical Informatics, the Ohio State University (e-mail:metin.gurcan@osumc.edu).

II. Data Collection

Preliminary data was obtained for a whole-slide FL case. Formalin fixed paraffin embedded (FFPE) tissue sections from healthy tonsil biopsies were used to generate image data as well as MS data because of the clear demarcations of the mantle zones in these images.

A. Tissue preparation

Serial 5 µm thick sections were cut from the FFPE tonsil tissue blocks using a microtome. Sections from the tissue blocks were either mounted onto ITO-coated conductive slides for MALDI MS analysis, or onto standard glass microscope slides for H&E staining. Deparafinization of the tissue sections was carried out using washes in xylene and graded ethanol washes. Once the slides were fully dry, a trypsin solution was automatically spotted onto the tissue section using a Portrait 630 reagent multi-spotter (Labcyte, Sunnyvale, CA) into an array incorporating 250 µm center to center spacing between individual spots, each of which were approximately 175 µm in diameter. The trypsin was spotted for over 30 iterations while allowing the trypsin solution to dry following each droplet application. An optically scanned image of the spotted tissue was generated for registration with the H&E stained tissue image. The spotted tissue image was used to map spatial locations of the spots in the tissue to the corresponding mass spectra. The spotted tissue image is relatively low resolution compared with the H&E image.

An H&E stained section of the FFPE tissue section was scanned to generate a high-resolution image of pixel size 59363 x 58311. This high-resolution image was scaled down by a factor of 15 for use in registration. Fig.1(a) shows a lower-resolution version of the H&E stained tissue image.

B. Imaging Mass Spectrometry

Following trypsin/matrix application, FFPE tonsil tissues were analyzed using an Ultraflex II MALDI TOF/TOF mass spectrometer (Bruker Daltonics, Billerica, MA) controlled by the Flex Control 3.0 software package. The mass spectrometer was operated with positive polarity in reflectron mode and spectra acquired in the range of m/z 700-5000. Image acquisition of the spotted arrays was carried out using the Flex Imaging 2.0 (Bruker Daltonics, Billerica, MA) software package. A total of 1600 spectra were acquired at each spot position in a customized spiral raster pattern in 200 shot increments at a laser frequency of 200 Hz. The customized raster pattern was used to sample the entire spot area. The red spots on the tissue shown in Fig. 1(b) indicate the locations where mass spectra were acquired. This data is critical to the analysis because it correlates spatial locations on the tissue section with a unique mass spectrum.

Fig. 1(a). Tissue image

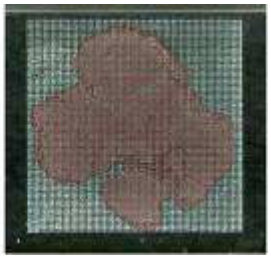

Fig. 1(b). Laser grid image

III. Image Analysis

A. Spot Detection

As shown in Fig. 1(b), the red locations indicating the laser spots are easily identifiable on the spotted tissue image. However, the image also contains non-red spots and the RGB colorspace is not optimal for locating the red spots.

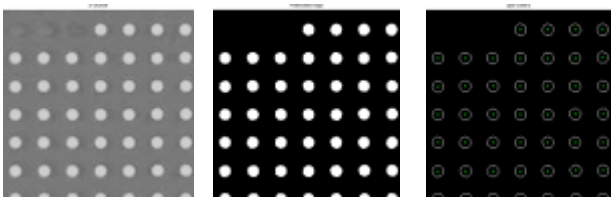

Fig. **2**. Laser spot detection: a* channel, Thresholded image, Final result

The spotted tissue image was first converted to the La*b* colorspace. The red spots in the RGB colorspace are converted to bright spots in the a* channel, while the gray-blue spots in the RGB colorspace are observed to have significantly lower values in the same channel. The a* channel was segmented into background and laser spots by thresholding, with the threshold determined using the Otsu method [16]. The segmentation operation is followed by a simple edge detection operation. Laser spots were detected by labeling connected components and computing the centroid of each connected component.

Once the laser spots were identified, the locations of the laser spots in the image were mapped to the files containing the MS data.

B. Image Registration

For the preliminary study, the scaled down H&E image and the laser grid image were registered manually. A non-reflective similarity transform was used after selecting appropriate control points in the two images. The registration process was completed using the Image Processing Toolbox in MATLAB (Mathworks, Natick, MA). The two images were registered after dividing them into four separate sub-images in order to localize the effects of distortion caused during the sectioning process.

Fig. 3(a). Tissue with laser circles

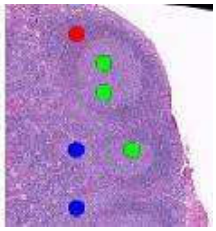

Fig. 3(b). Sample points from regions of interest

IV. MALDI-MS Data Analysis

A. Data Selection

In order to characterize different sections of the tissue that are morphologically relevant to disease state, it was first necessary to identify mantle, follicle and intra-follicular regions of the tissue as shown in Fig. 3(b). The red location corresponds to the mantle zone, green corresponds to the follicle and blue corresponds to the intra-follicular region. Fig.4 shows a sample spectrum obtained from a mantle zone location. The locations of laser spots were transferred to the H&E stained image as shown in Fig. 3(a). An expert hematopathologist (GL) reviewed these locations and established the ground truth for the subsequent analysis. Data points that were not located in the mantle, follicle or intrafollicle regions were not used in the analysis because they are not considered relevant to the disease state.

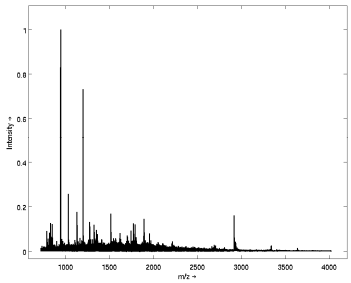

Fig. 4. Sample spectrum from mantle zone in tissue

B. Analysis

MS data from the selected points of interest was first baseline corrected for noise and background reduction and then normalized. Previous studies have compared mass spectra from normal and disease tissue to identify significant bio-markers. Since a single normal tissue sample was used in the study, significant bio-markers could not be identified by simple comparison of protein profiles from different tissue sections. Therefore, the complete spectra consisting of 56,492 data points each were used to develop classifiers to distinguish between the three tissue regions. Common statistical techniques applied for the analysis and classification of mass spectrometry data are Principle Component Analysis (PCA), Support Vector Machines (SVM) and K-Nearest Neighbor classification [8], [13-15].

In this study we used the Support Vector Machine (SVM) and K-Nearest Neighbor (KNN) classifiers available in the Statistics Toolbox for MATLAB [17]. A leave-one-out cross validation study was performed using the SVM and KNN classifiers. The results are summarized in Table 1 and 2.

Ground Truth / Computer	Mantle	Follicle	Intrafollicle
Mantle	40.00	4.00	56.00
Follicle	23.52	64.70	11.76
Intrafollicle	4.46	2.23	93.29

Table 1 Confusion matrix in % for leave one out validation using SVM classifier

Ground Truth / Computer	Mantle	Follicle	Intrafollicle
Mantle	40.00	24.00	36.00
Follicle	47.05	52.94	0
Intrafollicle	11.17	4.46	84.35

Table 2 Confusion matrix in % for leave one out validation using KNN classifier

A second analysis similar to the procedure described by Ressom et al in [8] was used to perform a K-fold cross validation study. The availability of data points from each class used in the analysis is dictated by the physical characteristics of the tissue being studied. As a result, in this study a total of 189 spectra from the intrafolliclular region were available as compared with 31 for the follicle regions and 43 for the mantle zone. To avoid biasing the classifiers, only 43 spectra from the intrafollicle region were used along with all the data from mantle and follicle regions. Tables 3 and 4 summarize the results of this analysis averaged over 200 runs of the K-fold cross validation procedure. In each run, training and testing sets were determined randomly, however, the total number of spectra from each class were the same. It is seen that both classifiers perform well in identifying the intrafollicle and mantle regions. However, the follicle regions are misclassified into the mantle zone almost 50% of the time.

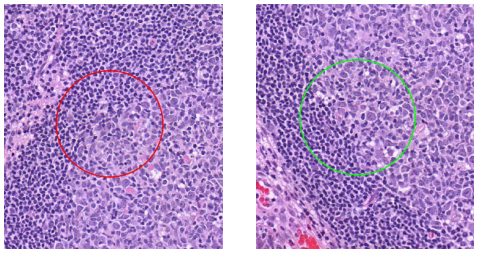

Figure 6. Classification challenges

A potential cause of the lower classification accuracy in the case of mantle vs. follicle is that in several cases, the mass spectrometry data was obtained from a region overlapping both the mantle zone and the follicle region as shown in Fig. 6.

Ground Truth / Computer	Mantle	Follicle	Intrafollicle
Mantle	85.55	9.55	4.90
Follicle	41.73	53.45	4.82
Intrafollicle	22.98	0.36	76.65

Table 3. Confusion matrix in % for SVM classifier

Ground Truth / Computer	Mantle	Follicle	Intrafollicle
Mantle	48.27	42.22	9.51
Follicle	45.56	50.98	3.46
Intrafollicle	20.22	4.26	75.52

Table 4. Confusion matrix in % for KNN classifier

In such cases, the data is assigned by the human expert to either one of the regions based on the location of a majority of the laser spot inside either one of the regions. This can affect the results of the classifier since the mass spectra now contains contributions from two regions of tissue. In Fig. 6, two regions classified as mantle (red) and follicle (green) respectively show this problem. The inability of the classifiers to distinguish between the mantle and follicle regions with high rates of accuracy can also be ascribed to the fact that these two regions of tissue consist of similar types of cells. As a result it is reasonable to expect that the protein profiles of these regions are similar in nature. In this study, all data points in each mass spectrum were considered in the analysis which makes the problem computationally expensive. However, the results from this pilot study may be used to identify significant markers that can be used for reducing the data dimensionality, thus allowing the problem to be reduced to a more tractable size.

V. Discussion

This paper describes a preliminary study that was done to assess the efficacy of using MALDI-MS for classifying regions of interest in a Follicular Lymphoma tissue sample. A more detailed and rigorous study involving larger data sets is currently being developed, which should lead to the development of classifiers for identifying follicle, mantle and intrafollicle regions in the tissue. Results of these studies will be used to develop protocols for classifying FL into appropriate classes (I, II, II) using mass spectrometry data as well as traditional morphological information used by pathology experts.

VI. Conclusion

In this paper, we have presented a systematic approach to enable the use of mass spectrometry data for Follicular Lymphoma grading. The proteomic data obtained from the MALDI-MS analysis was used to classify locations on a tissue into disease relevant classes. By combining the results of the MS analysis with computer-aided image analysis it may be possible to develop a novel diagnostic tool that combines both molecular and morphological datasets from a tissue to give a more accurate diagnosis and classification of Follicular Lymphoma.

References

[1] E. S. Jaffe, N. L. Harris, H. Stein, and J. W. Vardiman, "World health organization classification of tumours of haematopoietic and lymphoid tissues," IARC Press, 2001.

[2] The Non-Hodgkin's Lymphoma Classification ,"A clinical evaluation of the international lymphoma study group classification of non-hodgkin's lymphoma.,", vol. 89, pp. 3909–3918, 1997.

[3] O. Sertel , J. Kong , U.V. Catalyurek , G. Lozanski , J. Saltz , M.N. Gurcan , "Histopathological image analysis using model-based intermediate representations and color texture: Follicular lymphoma grading," Journal of Signal Processing Systems, v. 55, n. 1-3, pp. 169-183, 2009

[4] O. Sertel , J. Kong J, G. Lozanski, U. Catalyurek , J. Saltz, M.N. Gurcan , "Computerized microscopic image analysis of follicular lymphoma," *SPIE Medical Imaging 2008*, 16 - 21 February 2008

[5] P. Chaurand, S.A. Schwartz, M. L. Reyzer, and R.M. Caprioli, "Imaging mass spectrometry: principles and potentials", Toxicologic Pathology, vol. 33, no. 1, pp. 92–101, 2005.

[6] P. Chaurand, M. E. Sanders, R.A. Jensen, and R. M. Caprioli, "Proteomics in diagnostic pathology : Profiling and imaging proteins directly in tissue sections," American Journal of Pathology., vol. 165, no.4, pp. 1057–1068, 2004.

[7] M. Stoeckli., P. Chaurand, D. E. Hallahan and R.M. Caprioli,"Imaging mass spectrometry: A new technology for the analysis of protein expression in mammalian tissues", Nat Med, 2001.

[8] H.W. Ressom, R.S. Varghese, E. Orvisky, S.K. Drake, G.L. Hortin, M. Abdel-Hamid, C.A. Loffredo, and R. Goldman, "Analysis of maldi-tof serum profiles for biomarker selection and sample classification," Computational Intelligence in Bioinformatics and Computational Biology, 2005. CIBCB '05. Proceedings of the 2005 IEEE Symposium on, pp. 1–7, Nov. 2005.

[9] M. L. Reyzer and R. M. Caprioli, "Maldi mass spectrometry for direct tissue analysis: A new tool for biomarker discovery," Journal of Proteome Research, vol. 4(4), pp. 1138–42, 2005.

[10] S. A. Schwartz, R. J. Weil, R. C. Thompson, Y.Shyr, J. H. Moore, S. A. Toms, M. D. Johnson, and R. M. Caprioli, "Proteomic-based prognosis of brain tumor patients using direct-tissue matrix-assisted laser desorption ionization mass spectrometry," Cancer Res, vol. 65, no. 17, pp. 7674–7681, 2005.

[11] D. S. Cornett, J. A. Mobley, E. C. Dias, M. Andersson, C. L. Arteaga, M. E. Sanders, and R. M. Caprioli, "A novel histology directed strategy for maldi-ms tissue profiling that improves throughput and cellular specificity in human breast cancer," Molecular and Cellular Proteomics, 2006.

[12] P. Chaurand, S. A. Schwartz, D. Billheimer, B. J. Xu, A. Crecelius, and R. M. Caprioli, "Integrating histology and imaging mass spectrometry," Analytical Chemistry, vol. 76, pp. 1145–1155, February 2004.

[13] M. R. Groseclose, P. P. Massion, P. Chaurand, and R. M. Caprioli, "High-throughput proteomic analysis of formalin-fixed paraffin-embedded tissue microarrays using maldi imaging mass spectrometry," Proteomics, vol. 8, pp. 3715–3724, 2008.

[14] M. E. Sanders, E.C. Dias, B. J. Xu, J. A. Mobley, D. Billheimer, H. Roder, J. Grigorieva, M. Dowsett, C. L. Arteaga, and R.M. Caprioli, "Differentiating proteomic biomarkers in breast cancer by laser capture microdissection and maldi ms," Journal of Proteome Research, vol. 7(4), pp. 1500–1507, 2008.

[15] M. Gerhard, S.O. Deininger, and F.-M. Schleif, "Statistical classification and visualization of maldi-imaging data," IEEE International Symposium on Computer-Based Medical Systems, 2007.

[16] N. Otsu, "A threshold selection method from gray-level histograms." *IEEE Transactions on Systems, Man and Cybernetics* , *9* (1), 62-66., 1979

[17] The MathWorks Inc, "Statistics Toolbox", http://www.mathworks.com/products/statistics/